

Search for lepton flavor violating τ decays into three leptons

Belle Collaboration

Y. Miyazaki^{t,*}, I. Adachi^g, H. Aihara^{an}, K. Arinstein^a, V. Aulchenko^a, T. Aushev^{p,k},
A.M. Bakich^{aj}, V. Balagura^k, E. Barberio^s, A. Bay^p, U. Bitenc^l, A. Bondar^a, A. Bozek^y,
M. Bračko^{g,r,l}, T.E. Browder^f, A. Chen^v, K.-F. Chen^x, W.T. Chen^v, B.G. Cheon^c, R. Chistov^k,
I.-S. Cho^{ar}, Y. Choi^{ai}, M. Dash^{aq}, A. Drutskoy^c, S. Eidelman^a, D. Epifanov^a, N. Gabyshev^a,
H. Haⁿ, J. Haba^g, K. Hara^t, K. Hayasaka^t, H. Hayashii^u, M. Hazumi^g, D. Heffernan^{ad}, Y. Hoshi^{al},
W.-S. Hou^x, Y.B. Hsiung^x, H.J. Hyun^o, T. Iijima^t, K. Inami^t, A. Ishikawa^{af}, R. Itoh^g, M. Iwasaki^{an},
Y. Iwasaki^g, D.H. Kah^o, H. Kaji^t, P. Kapusta^y, H. Kawai^b, T. Kawasaki^{aa}, H. Kichimi^g, H.J. Kim^o,
Y.J. Kim^d, K. Kinoshita^c, Y. Kozakai^t, P. Križan^{q,l}, P. Krokovny^g, R. Kumar^{ae}, C.C. Kuo^v,
A. Kuzmin^a, Y.-J. Kwon^{ar}, J.S. Lee^{ai}, M.J. Lee^{ah}, S.E. Lee^{ah}, S.-W. Lin^x, Y. Liu^d, D. Liventsev^k,
F. Mandl^j, S. McOnie^{aj}, W. Mitaroff^j, H. Miyake^{ad}, H. Miyata^{aa}, R. Mizuk^k, D. Mohapatra^{aq},
G.R. Moloney^s, T. Mori^t, T. Nagamine^{am}, E. Nakano^{ac}, M. Nakao^g, H. Nakazawa^v, Z. Natkaniec^y,
S. Nishida^g, O. Nitoh^{ap}, S. Noguchi^u, S. Ogawa^{ak}, T. Ohshima^t, S. Okuno^m, S.L. Olsen^{f,h},
H. Ozaki^g, P. Pakhlov^k, G. Pakhlova^k, C.W. Park^{ai}, H. Park^o, K.S. Park^{ai}, R. Pestotnik^l,
L.E. Piilonen^{aq}, A. Poluektov^a, Y. Sakai^g, O. Schneider^p, A.J. Schwartz^c, K. Senyo^t, M.E. Seviour^s,
M. Shapkinⁱ, H. Shibuya^{ak}, J.-G. Shiu^x, B. Shwartz^a, A. Sokolovⁱ, A. Somov^c, S. Stanič^{ab},
M. Starič^l, T. Sumiyoshi^{ao}, F. Takasaki^g, N. Tamura^{aa}, M. Tanaka^g, G.N. Taylor^s, Y. Teramoto^{ac},
I. Tikhomirov^k, S. Uehara^g, K. Ueno^x, Y. Unno^e, S. Uno^g, P. Urquijo^s, Y. Usov^a, G. Varner^f,
S. Villa^p, A. Vinokurova^a, C.H. Wang^w, P. Wang^h, X.L. Wang^h, Y. Watanabe^m, E. Wonⁿ,
Y. Yamashita^z, Z.P. Zhang^{ag}, V. Zhilich^a, A. Zupanc^l, O. Zyukova^a

^a Budker Institute of Nuclear Physics, Novosibirsk, Russia

^b Chiba University, Chiba, Japan

^c University of Cincinnati, Cincinnati, OH, USA

^d The Graduate University for Advanced Studies, Hayama, Japan

^e Hanyang University, Seoul, South Korea

^f University of Hawaii, Honolulu, HI, USA

^g High Energy Accelerator Research Organization (KEK), Tsukuba, Japan

^h Institute of High Energy Physics, Chinese Academy of Sciences, Beijing, PR China

ⁱ Institute for High Energy Physics, Protvino, Russia

^j Institute of High Energy Physics, Vienna, Austria

^k Institute for Theoretical and Experimental Physics, Moscow, Russia

^l J. Stefan Institute, Ljubljana, Slovenia

^m Kanagawa University, Yokohama, Japan

ⁿ Korea University, Seoul, South Korea

^o Kyungpook National University, Taegu, South Korea

^p École Polytechnique Fédérale de Lausanne, EPFL, Lausanne, Switzerland

^q Faculty of Mathematics and Physics, University of Ljubljana, Ljubljana, Slovenia

^r University of Maribor, Maribor, Slovenia

^s University of Melbourne, Victoria, Australia

^t Nagoya University, Nagoya, Japan

^u Nara Women's University, Nara, Japan

^v National Central University, Chung-li, Taiwan

- ^w National United University, Miao Li, Taiwan
^x Department of Physics, National Taiwan University, Taipei, Taiwan
^y H. Niewodniczanski Institute of Nuclear Physics, Krakow, Poland
^z Nippon Dental University, Niigata, Japan
^{aa} Niigata University, Niigata, Japan
^{ab} University of Nova Gorica, Nova Gorica, Slovenia
^{ac} Osaka City University, Osaka, Japan
^{ad} Osaka University, Osaka, Japan
^{ae} Panjab University, Chandigarh, India
^{af} Saga University, Saga, Japan
^{ag} University of Science and Technology of China, Hefei, PR China
^{ah} Seoul National University, Seoul, South Korea
^{ai} Sungkyunkwan University, Suwon, South Korea
^{aj} University of Sydney, Sydney, NSW, Australia
^{ak} Toho University, Funabashi, Japan
^{al} Tohoku Gakuin University, Tagajo, Japan
^{am} Tohoku University, Sendai, Japan
^{an} Department of Physics, University of Tokyo, Tokyo, Japan
^{ao} Tokyo Metropolitan University, Tokyo, Japan
^{ap} Tokyo University of Agriculture and Technology, Tokyo, Japan
^{aq} Virginia Polytechnic Institute and State University, Blacksburg, VA, USA
^{ar} Yonsei University, Seoul, South Korea

Received 23 December 2007; accepted 23 December 2007

Available online 9 January 2008

Editor: M. Doser

Abstract

We search for lepton flavor violating τ decays into three leptons (electron or muon) using 535 fb^{-1} of data collected with the Belle detector at the KEKB asymmetric-energy e^+e^- collider. No evidence for these decays is observed, and we set 90% confidence level upper limits on the branching fractions of $(2.0\text{--}4.1) \times 10^{-8}$. These results improve upon our previously published upper limits by factors of 4.9 to 10.

© 2008 Elsevier B.V. All rights reserved.

PACS: 11.30.Fs; 13.35.Dx; 14.60.Fg

1. Introduction

Lepton flavor violation (LFV) appears in various extensions of the Standard Model (SM). In particular, lepton flavor violating decays $\tau^- \rightarrow \ell^- \ell^+ \ell^-$ (where $\ell = e$ or μ)¹ are discussed in various supersymmetry models [1–7], models with little Higgs [8,9], left–right symmetric models [10], as well as models with heavy singlet Dirac neutrinos [11] and very light pseudoscalar bosons [12]. Some of these models with certain combinations of parameters predict that the branching fractions for $\tau^- \rightarrow \ell^- \ell^+ \ell^-$ can be as high as 10^{-7} , which is already accessible in high-statistics B factory experiments. Searches for LFV τ decays into three leptons have a long history [13] beginning from the pioneering experiment of MARKII [14]. In previous analyses, both Belle and BaBar reached 90% confidence level (C.L.) upper limits on the branching fractions at the 10^{-7} level [15,16], based on about 90 fb^{-1} of data. The BaBar Collaboration has recently used 376 fb^{-1} of data to ob-

tain 90% C.L. upper limits in the range $(3.7\text{--}8.0) \times 10^{-8}$ [17]. Here, we update our previous results with a much larger data set (535 fb^{-1}) collected with the Belle detector at the KEKB asymmetric-energy e^+e^- collider [18], taken at the $\Upsilon(4S)$ resonance and 60 MeV below it.

The Belle detector is a large-solid-angle magnetic spectrometer that consists of a silicon vertex detector (SVD), a 50-layer central drift chamber (CDC), an array of aerogel threshold Cherenkov counters (ACC), a barrel-like arrangement of time-of-flight scintillation counters (TOF), and an electromagnetic calorimeter comprised of CsI(Tl) crystals (ECL), all located inside a superconducting solenoid coil that provides a 1.5 T magnetic field. An iron flux-return located outside the coil is instrumented to detect K_L^0 mesons and to identify muons (KLM). The detector is described in detail elsewhere [19].

Leptons are identified using likelihood ratios calculated from the response of various subsystems of the detector. For electron identification, the likelihood ratio is defined as $\mathcal{P}(e) = \mathcal{L}_e / (\mathcal{L}_e + \mathcal{L}_x)$, where \mathcal{L}_e and \mathcal{L}_x are the likelihoods for electron and non-electron, respectively, determined using the ratio of the energy deposit in the ECL to the momentum measured in the SVD and CDC, the shower shape in the ECL, the matching between the position of the charged track trajectory and the cluster

* Corresponding author.

E-mail address: miya@hepl.phys.nagoya-u.ac.jp (Y. Miyazaki).

¹ Throughout this Letter, charge-conjugate modes are implied unless stated otherwise.

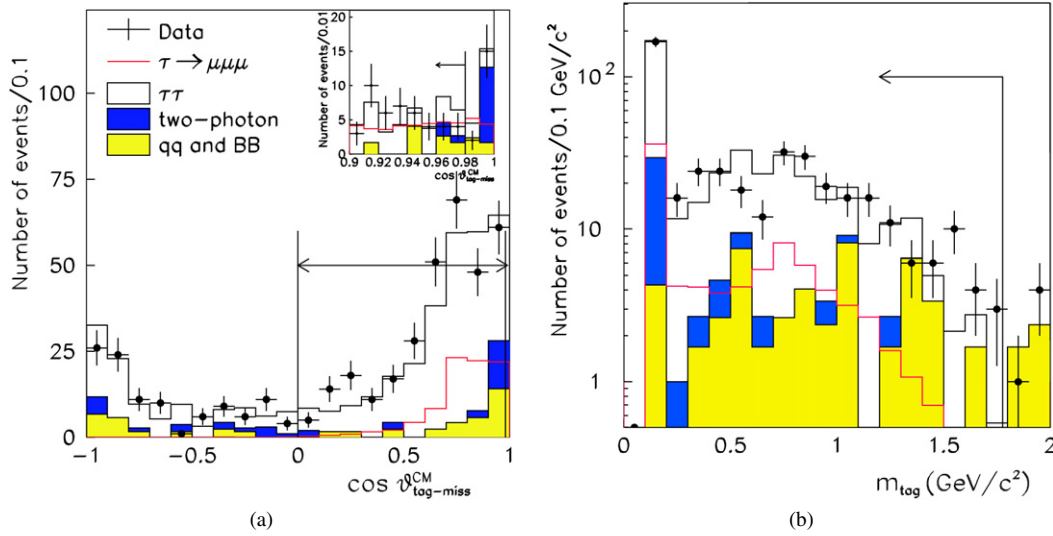


Fig. 1. Kinematic distributions used in the event selection after applying $E_{\text{vis}}^{\text{CM}}$ and T cuts: (a) the cosine of the opening angle between a charged track on the tag side and missing particles in the CM system ($\cos\theta_{\text{tag-miss}}^{\text{CM}}$); (b) the reconstructed mass on the tag side using a charged track and photons. The signal MC ($\tau^- \rightarrow \mu^- \mu^+ \mu^-$) distributions with arbitrary normalization are shown for comparison; the background MC distributions are normalized to the data luminosity. Selected regions are indicated by the arrows from the marked cut boundaries.

position in the ECL, the hit information from the ACC, and the dE/dx information in the CDC [20]. For muon identification, the likelihood ratio is defined as $\mathcal{P}(\mu) = \mathcal{L}_\mu / (\mathcal{L}_\mu + \mathcal{L}_\pi + \mathcal{L}_K)$, where \mathcal{L}_μ , \mathcal{L}_π and \mathcal{L}_K are the likelihoods for the muon, pion and kaon hypotheses, respectively, based on the matching quality and penetration depth of associated hits in the KLM [21].

In order to estimate the signal efficiency and to optimize the event selection, we use Monte Carlo (MC) samples. The signal and the background events from generic $\tau^+\tau^-$ decays are generated by KKMC/TAUOLA [22]. In the signal MC, we generate $\tau^+\tau^-$, where a τ decays into three leptons using a 3-body-phase-space model [23], and the other τ decays generically. Other backgrounds, including $B\bar{B}$ and $e^+e^- \rightarrow q\bar{q}$ ($q = u, d, s, c$) events, Bhabha events, $e^+e^- \rightarrow \mu^+\mu^-$, and two-photon processes are generated by EvtGen [24], BHLUMI [25], KKMC and AAFH [26], respectively. All kinematic variables are calculated in the laboratory frame unless otherwise specified. In particular, variables calculated in the e^+e^- center-of-mass (CM) system are indicated by the superscript “CM”.

2. Event selection

We search for $\tau^+\tau^-$ events in which one τ (the signal τ) decays into three leptons, and the other τ (the tag τ) decays into one charged track, any number of additional photons and neutrinos. Candidate τ -pair events are required to have four tracks with zero net charge. The following final states are considered: $e^-e^+e^-$, $\mu^- \mu^+ \mu^-$, $e^- \mu^+ \mu^-$, $\mu^- e^+ e^-$, $e^+ \mu^- \mu^-$, and $\mu^+ e^- e^-$. The event selection is optimized mode-by-mode since the backgrounds are mode dependent.

The event selection starts by reconstructing four charged tracks and any number of photons within the fiducial volume defined by $-0.866 < \cos\theta < 0.956$, where θ is the polar angle relative to the direction opposite to that of the incident e^+ beam in the laboratory frame. The transverse momentum (p_t) of each

charged track and the energy of each photon (E_γ) are required to satisfy $p_t > 0.1$ GeV/ c and $E_\gamma > 0.1$ GeV, respectively. For each charged track, the distance of the closest point with respect to the interaction point is required to be less than ± 0.5 cm in the transverse direction and less than ± 3.0 cm in the longitudinal direction.

Using the plane perpendicular to the CM thrust axis [27], which is calculated from the observed tracks and photon candidates, we separate the particles in an event into two hemispheres. These are referred to as the signal and tag sides. The tag side contains one charged track while the signal side contains three charged tracks. We require all charged tracks on the signal side to be identified as leptons. The electron (muon) identification criteria are $\mathcal{P}(e) > 0.9$ ($\mathcal{P}(\mu) > 0.9$) and momentum greater than 0.3 GeV/ c (0.6 GeV/ c). The electron (muon) identification efficiency is 91% (85%) while the probability to misidentify a pion as an electron (a muon) is below 0.5% (2%).

To ensure that the missing particles are neutrinos rather than photons or charged particles that pass outside the detector acceptance, we impose requirements on the missing momentum \vec{p}_{miss} , which is calculated by subtracting the vector sum of the momenta of all tracks and photons from the sum of the e^+ and e^- beam momenta. We require that the magnitude of \vec{p}_{miss} be greater than 0.4 GeV/ c , and that its direction point into the fiducial volume of the detector.

To reject $q\bar{q}$ background, we require that the magnitude of thrust (T) be $0.90 < T < 0.97$ for all modes except for the $\tau^- \rightarrow e^- e^+ e^-$ mode, for which it is $0.90 < T < 0.96$. We also require $5.29 \text{ GeV} < E_{\text{vis}}^{\text{CM}} < 9.5 \text{ GeV}$, where $E_{\text{vis}}^{\text{CM}}$ is the total visible energy in the CM system, defined as the sum of the energies of the three leptons, the charged track on the tag side (with a pion mass hypothesis), and all photon candidates.

Since neutrinos are emitted only on the tag side, the direction of \vec{p}_{miss} should lie within the tag side of the event. The cosine of the opening angle between \vec{p}_{miss} and the charged track on

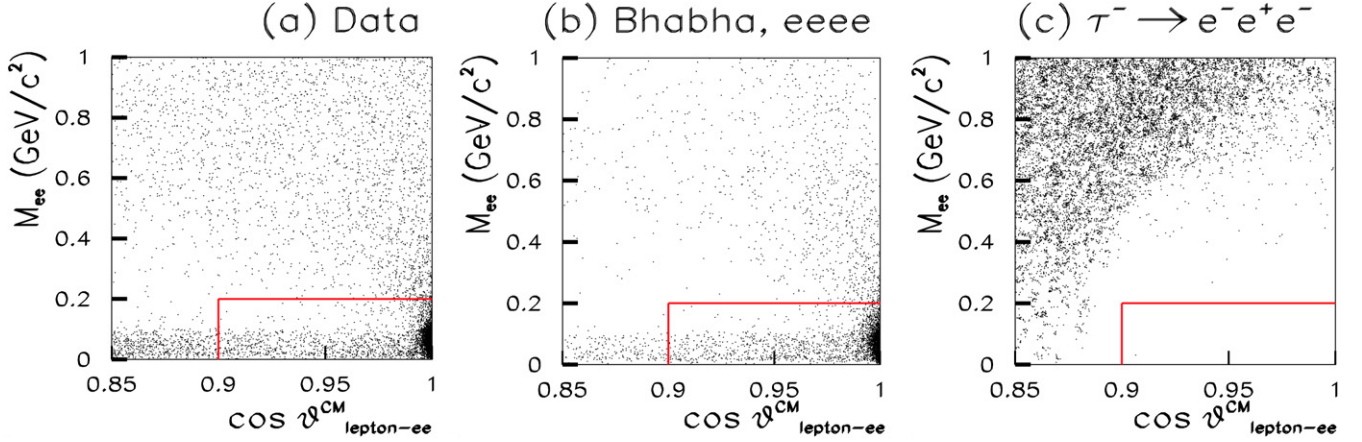


Fig. 2. Scatter-plots of the reconstructed invariant mass of the e^+e^- pair (M_{ee}) vs. cosine of the opening angle between the direction of the e^+e^- pair and the other electron ($\cos\theta_{\text{lepton-}ee}^{\text{CM}}$) for (a) data, (b) Bhabha and $eeee$, (c) signal MC ($\tau^- \rightarrow e^-e^+e^-$).

the tag side in the CM system, $\cos\theta_{\text{tag-miss}}^{\text{CM}}$, is required to lie in the range $0.0 < \cos\theta_{\text{tag-miss}}^{\text{CM}} < 0.98$. This upper limit reduces background from Bhabha, $\mu^+\mu^-$ and two-photon background events, as radiated gammas from the tag-side track result in missing momentum if they overlap with the ECL clusters of the tag-side track [28]. The reconstructed mass on the tag side using a charged track (with a pion mass hypothesis) and photons, m_{tag} , is required to be less than $1.777 \text{ GeV}/c^2$. As shown in Fig. 1, reasonable agreement between data and the background expectation from MC simulation is obtained in the distributions of $\cos\theta_{\text{tag-miss}}^{\text{CM}}$ and m_{tag} .

Conversions ($\gamma \rightarrow e^+e^-$) are a large background for the $\tau^- \rightarrow e^-e^+e^-$ and $\mu^-e^+e^-$ modes. For these modes, if the invariant mass of the e^+e^- pair (M_{ee}) is less than $0.2 \text{ GeV}/c^2$, we require that the cosine of the opening angle in the CM system between the momentum of the e^+e^- pair and the momentum of the other lepton ($\cos\theta_{\text{lepton-}ee}^{\text{CM}}$) be less than 0.90. We retain the region, $M_{ee} < 0.2 \text{ GeV}/c^2$, $0.85 < \cos\theta_{\text{lepton-}ee}^{\text{CM}} < 0.90$ in order not to suppress signal events with small M_{ee} , which are possible in some models beyond the SM. As shown in Fig. 2 for the $\tau^- \rightarrow e^-e^+e^-$ mode (two entries for each event), the signal efficiency is not affected by this cut, while the large background from conversions is substantially reduced.

For the $\tau^- \rightarrow e^-e^+e^-$ and $\tau^- \rightarrow e^-\mu^+\mu^-$ modes, the charged track on the tag side is required not to be an electron by applying $\mathcal{P}(e) < 0.1$; this reduces large backgrounds from two-photon and Bhabha processes that remain. Furthermore, we reject events if the charged track on the tag side traverses the gap between the barrel and the endcap of the ECL. To reduce Bhabha and $\mu^+\mu^-$ backgrounds, we require that the momentum in the CM system of the charged track on the tag side be less than $4.5 \text{ GeV}/c$ for the $\tau^- \rightarrow e^-e^+e^-$ and $\tau^- \rightarrow \mu^-e^+e^-$ modes.

Finally, to suppress backgrounds from generic $\tau^+\tau^-$ and $q\bar{q}$ events, we apply a selection based on the magnitude of the missing momentum p_{miss} and the missing mass squared m_{miss}^2 for all modes except for $\tau^- \rightarrow e^+\mu^-\mu^-$ and $\mu^+e^-e^-$. We do not apply this cut for the latter two modes since backgrounds in these

Table 1

The selection criteria for the missing momentum (p_{miss}) and missing mass squared (m_{miss}^2) for each mode. The units for p_{miss} and m_{miss}^2 are GeV/c and $(\text{GeV}/c^2)^2$, respectively

Mode	Hadronic tag mode	Leptonic tag mode
$\tau^- \rightarrow e^-e^+e^-$	$p_{\text{miss}} > -3.0m_{\text{miss}}^2 - 1.0$ $p_{\text{miss}} > 4.2m_{\text{miss}}^2 - 1.5$	$p_{\text{miss}} > -2.5m_{\text{miss}}^2$ $p_{\text{miss}} > 2.0m_{\text{miss}}^2 - 1$
$\tau^- \rightarrow \mu^-\mu^+\mu^-$	$p_{\text{miss}} > -3.0m_{\text{miss}}^2 - 1.0$	$p_{\text{miss}} > -2.5m_{\text{miss}}^2$
$\tau^- \rightarrow e^-\mu^+\mu^-$	$p_{\text{miss}} > 3.0m_{\text{miss}}^2 - 1.5$	$p_{\text{miss}} > 1.3m_{\text{miss}}^2 - 1$
$\tau^- \rightarrow \mu^-e^+e^-$		
$\tau^- \rightarrow e^+\mu^-\mu^-$	Not applied	Not applied
$\tau^- \rightarrow \mu^+e^-e^-$		

cases are much smaller. We apply different selection criteria according to the lepton identification of the charged track on the tag side, as the number of emitted neutrinos is two if the track is an electron or muon (leptonic tag) while it is one if the track is a hadron (hadronic tag). The selection criteria are listed in Table 1; the distributions of m_{miss}^2 and p_{miss} for hadronic and leptonic decays are shown in Fig. 3.

3. Signal and background estimation

The signal candidates are examined in the two-dimensional plot of the $\ell^-\ell^+\ell^-$ invariant mass ($M_{3\ell}$) versus the difference of their energy from the beam energy in the CM system (ΔE). A signal event should have $M_{3\ell}$ close to the τ -lepton mass and ΔE close to zero. For all modes, the $M_{3\ell}$ and ΔE resolutions are parameterized from fits to the signal MC distributions, with an asymmetric Gaussian function that takes into account initial-state radiation. The resolutions in $M_{3\ell}$ and ΔE for each mode are summarized in Table 2.

To evaluate the branching fractions, we use elliptical signal regions that contain 90% of the MC signal events satisfying all selection criteria. We blind the data in the signal region until all selection criteria are finalized so as not to bias our choice of selection criteria. Figure 4 shows scatter-plots for the data and the signal MC distributed over $\pm 20\sigma$ in the $M_{3\ell} - \Delta E$ plane. No events are observed outside the signal region for

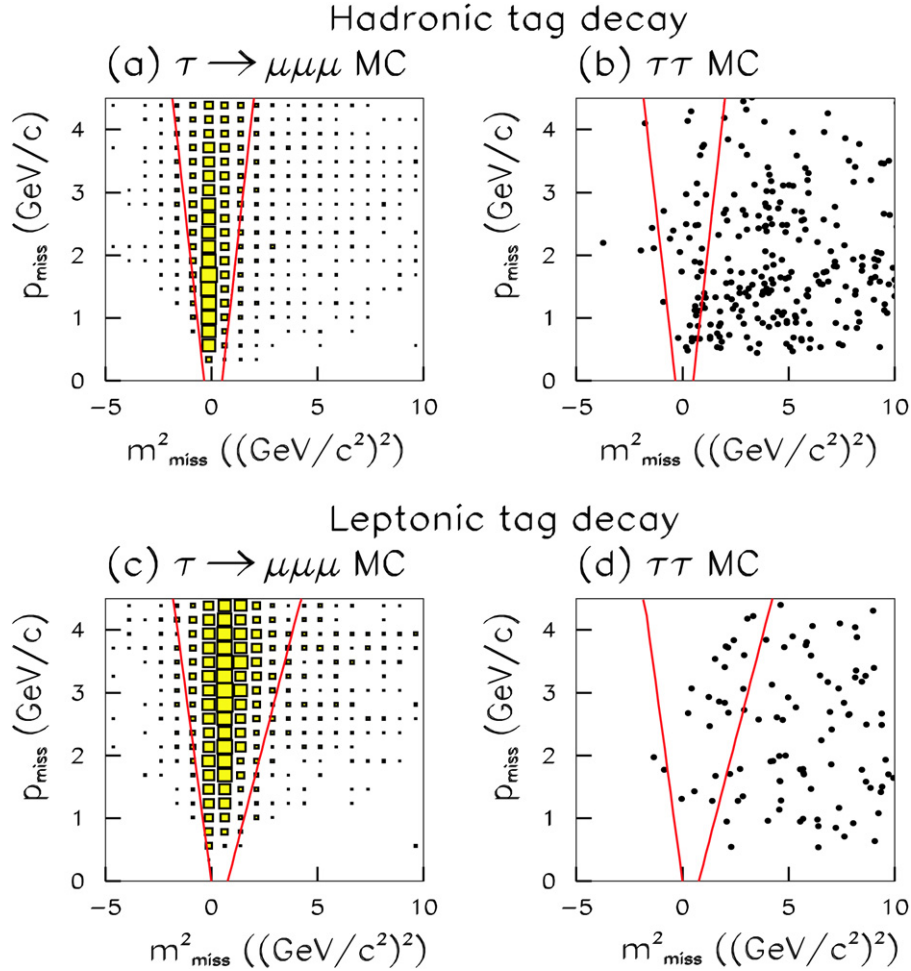


Fig. 3. Scatter-plots of p_{miss} vs. m_{miss}^2 : (a) and (b) show the signal MC ($\tau^- \rightarrow \mu^- \mu^+ \mu^-$) and the generic $\tau^+ \tau^-$ MC distributions, respectively, for the hadronic tags, while (c) and (d) show the same distributions for the leptonic tags. Selected regions are indicated by lines.

Table 2

Summary of $M_{3\ell}$ and ΔE resolutions. The σ^{high} (σ^{low}) means the standard deviation on the higher (lower) side of the peak

Mode	$\sigma_{M_{3\ell}}^{\text{high}}$ (MeV/c ²)	$\sigma_{M_{3\ell}}^{\text{low}}$ (MeV/c ²)	$\sigma_{\Delta E}^{\text{high}}$ (MeV)	$\sigma_{\Delta E}^{\text{low}}$ (MeV)
$\tau^- \rightarrow e^- e^+ e^-$	5.1	7.8	13.4	25.1
$\tau^- \rightarrow \mu^- \mu^+ \mu^-$	4.8	5.4	12.5	15.7
$\tau^- \rightarrow e^- \mu^+ \mu^-$	5.1	5.6	12.1	19.6
$\tau^- \rightarrow \mu^- e^+ e^-$	5.0	6.6	13.4	21.3
$\tau^- \rightarrow e^+ \mu^- \mu^-$	5.0	6.0	13.3	19.9
$\tau^- \rightarrow \mu^+ e^- e^-$	5.4	6.7	13.8	23.0

any modes except for $\tau^- \rightarrow e^- e^+ e^-$, in which four events are found. These remaining events all have $e^+ e^-$ invariant masses below 0.1 GeV/c², and we nominally attribute them to Bhabha electron or $\tau^- \rightarrow e^- \nu_\tau \bar{\nu}_e$ processes accompanied by a gamma conversion. The final estimate of background is based on the data with looser selection criteria for particle identification and event selection in the $M_{3\ell}$ sideband region. The sideband region is defined as the box inside the horizontal lines but excluding the signal region, as shown by the lines in Fig. 4. Assuming that the background distribution is uniform in the sideband region, the number of background events in the signal box is estimated by interpolating the number of observed events in the

Table 3

The signal efficiency (ε), the number of the expected background events (N_{BG}) estimated from the sideband data, total systematic uncertainty (σ_{syst}), the number of the observed events in the signal region (N_{obs}), 90% C.L. upper limit on the number of signal events including systematic uncertainties (s_{90}) and 90% C.L. upper limit on the branching fraction (\mathcal{B}) for each individual mode

Mode	ε (%)	N_{BG}	σ_{syst} (%)	N_{obs}	s_{90}	$\mathcal{B} (\times 10^{-8})$
$\tau^- \rightarrow e^- e^+ e^-$	6.00	0.40 ± 0.30	9.8	0	2.10	3.6
$\tau^- \rightarrow \mu^- \mu^+ \mu^-$	7.64	0.07 ± 0.05	7.4	0	2.41	3.2
$\tau^- \rightarrow e^- \mu^+ \mu^-$	6.08	0.05 ± 0.03	9.5	0	2.44	4.1
$\tau^- \rightarrow \mu^- e^+ e^-$	9.29	0.04 ± 0.04	7.8	0	2.43	2.7
$\tau^- \rightarrow e^+ \mu^- \mu^-$	10.8	0.02 ± 0.02	7.6	0	2.44	2.3
$\tau^- \rightarrow \mu^+ e^- e^-$	12.5	0.01 ± 0.01	7.7	0	2.46	2.0

sideband region into the signal region. The signal efficiency and the number of expected background events for each mode are summarized in Table 3. After estimating the background, we unblind and find no candidate events for any of the modes.

We estimate systematic uncertainties due to lepton identification, charged track finding, MC statistics, and integrated luminosity. The uncertainty due to the trigger efficiency is negligible compared with the other uncertainties. The uncertainties due to lepton identification are 2.2% per electron and 2.0% per muon. The uncertainty due to the charged track finding is es-

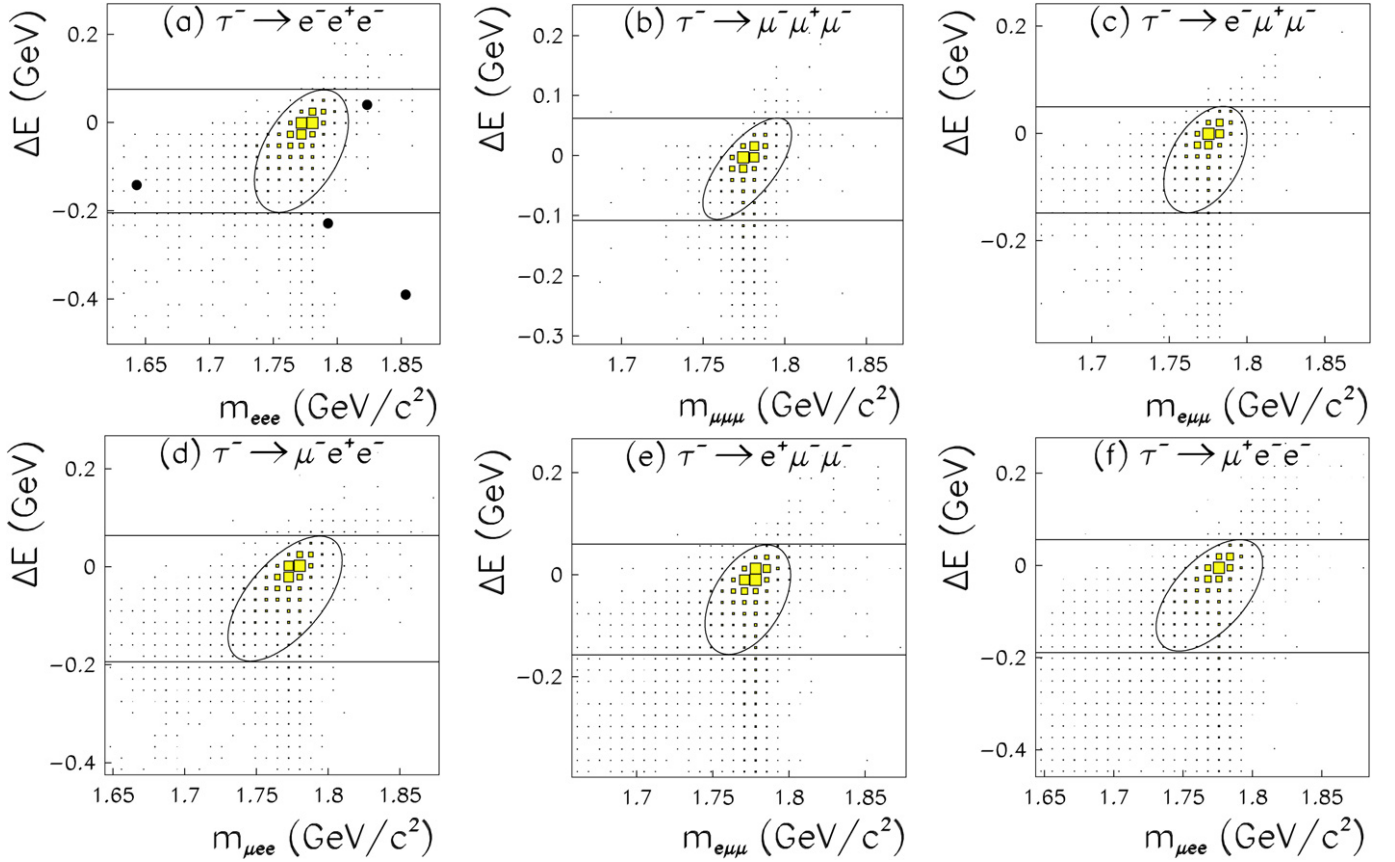


Fig. 4. Scatter-plots in the $M_{3\ell}-\Delta E$ plane: (a), (b), (c), (d), (e) and (f) correspond to the $\pm 20\sigma$ area for the $\tau^- \rightarrow e^- e^+ e^-$, $\tau^- \rightarrow \mu^- \mu^+ \mu^-$, $\tau^- \rightarrow e^- \mu^+ \mu^-$, $\tau^- \rightarrow \mu^- e^+ e^-$, $\tau^- \rightarrow e^+ \mu^- \mu^-$ and $\tau^- \rightarrow \mu^+ e^- e^-$ modes, respectively. The data are indicated by the solid circles. The filled boxes show the MC signal distribution with arbitrary normalization. The elliptical signal regions shown by a solid curve are used for evaluating the signal yield. The region between the horizontal solid lines excluding the signal region is used to estimate the expected background in the elliptical region from data with looser selection criteria.

estimated to be 1.0% per charged track. The uncertainty due to the e -veto on the tag side applied for the $\tau^- \rightarrow e^- e^+ e^-$ and $\tau^- \rightarrow e^- \mu^+ \mu^-$ modes is estimated to be the same as the uncertainty due to the electron identification. The uncertainties due to MC statistics and luminosity are estimated to be (0.5–0.9)% and 1.4%, respectively. All these uncertainties are added in quadrature, and the total systematic uncertainty for each mode is listed in Table 3.

4. Upper limits on the branching fractions

We set upper limits on the branching fractions of $\tau^- \rightarrow \ell^- \ell^+ \ell^-$ based on the Feldman–Cousins method [29]. The 90% C.L. upper limit on the number of the signal events and including a systematic uncertainty (s_{90}) is obtained using the POLE program without conditioning [30] based on the number of expected background events, observed data and the systematic uncertainty. The upper limit on the branching fraction (\mathcal{B}) is then given by

$$\mathcal{B}(\tau^- \rightarrow \ell^- \ell^+ \ell^-) < \frac{s_{90}}{2N_{\tau\tau}\varepsilon}, \quad (1)$$

where $N_{\tau\tau}$ is the number of $\tau^+\tau^-$ pairs, and ε is the signal efficiency. The value $N_{\tau\tau} = 492 \times 10^6$ is obtained from the integrated luminosity times the cross section of τ -pair production, which is calculated in the updated version of KKMC [31] to

be $\sigma_{\tau\tau} = 0.919 \pm 0.003$ nb. The 90% C.L. upper limits on the branching fractions $\mathcal{B}(\tau^- \rightarrow \ell^- \ell^+ \ell^-)$ are in the range between 2.0×10^{-8} and 4.1×10^{-8} and are summarized in Table 3. These results improve upon our previously published upper limits [15] by factors of 4.9 to 10. They are also more stringent upper limits than the recent BaBar results [17], except for the $\tau^- \rightarrow e^- \mu^+ \mu^-$ mode, for which the limit is similar.

5. Summary

We have searched for lepton flavor violating τ decays into three leptons using 535 fb^{-1} of data. No events are observed and we set 90% C.L. upper limits on the branching fractions: $\mathcal{B}(\tau^- \rightarrow e^- e^+ e^-) < 3.6 \times 10^{-8}$, $\mathcal{B}(\tau^- \rightarrow \mu^- \mu^+ \mu^-) < 3.2 \times 10^{-8}$, $\mathcal{B}(\tau^- \rightarrow e^- \mu^+ \mu^-) < 4.1 \times 10^{-8}$, $\mathcal{B}(\tau^- \rightarrow \mu^- e^+ e^-) < 2.7 \times 10^{-8}$, $\mathcal{B}(\tau^- \rightarrow e^+ \mu^- \mu^-) < 2.3 \times 10^{-8}$ and $\mathcal{B}(\tau^- \rightarrow \mu^+ e^- e^-) < 2.0 \times 10^{-8}$. These results improve upon our previously published upper limits by factors of 4.9 to 10. These more stringent upper limits can be used to constrain the space of parameters in various models of new physics.

Acknowledgements

The authors are grateful to A. Buras and Th. Mannel for fruitful discussions. We thank the KEKB group for the excel-

lent operation of the accelerator, the KEK cryogenics group for the efficient operation of the solenoid, and the KEK computer group and the National Institute of Informatics for valuable computing and Super-SINET network support. We acknowledge support from the Ministry of Education, Culture, Sports, Science, and Technology of Japan and the Japan Society for the Promotion of Science; the Australian Research Council and the Australian Department of Education, Science and Training; the National Science Foundation of China and the Knowledge Innovation Program of the Chinese Academy of Sciences under contract No. 10575109 and IHEP-U-503; the Department of Science and Technology of India; the BK21 program of the Ministry of Education of Korea, the CHEP SRC program and Basic Research program (grant No. R01-2005-000-10089-0) of the Korea Science and Engineering Foundation, and the Pure Basic Research Group program of the Korea Research Foundation; the Polish State Committee for Scientific Research; the Ministry of Education and Science of the Russian Federation and the Russian Federal Agency for Atomic Energy; the Slovenian Research Agency; the Swiss National Science Foundation; the National Science Council and the Ministry of Education of Taiwan; and the US Department of Energy.

References

- [1] J.R. Ellis, et al., *Phys. Rev. D* 66 (2002) 115013.
- [2] J.P. Saha, A. Kundu, *Phys. Rev. D* 66 (2002) 054021.
- [3] A. Brignole, et al., *Phys. Lett. B* 566 (2003) 217.
- [4] A. Brignole, A. Rossi, *Nucl. Phys. B* 701 (2004) 3.
- [5] R. Barbier, et al., *Phys. Rep. B* 420 (2005) 1.
- [6] P. Paradisi, *JHEP* 0510 (2005) 006.
- [7] E. Arganda, M.J. Herrero, *Phys. Rev. D* 73 (2006) 055003.
- [8] M. Blanke, et al., *JHEP* 0705 (2007) 013.
- [9] C.-X. Yue, Sh. Zhao, *Eur. Phys. J. C* 50 (2007) 897.
- [10] A.G. Akeroyd, et al., *Phys. Rev. D* 76 (2007) 013004.
- [11] A. Ilakovac, *Phys. Rev. D* 62 (2000) 036010.
- [12] A. Cordero-Cid, et al., *Phys. Rev. D* 72 (2005) 117701.
- [13] W.-M. Yao, et al., Particle Data Group, *J. Phys. G* 33 (2006) 1.
- [14] K.G. Hayes, et al., Mark II Collaboration, *Phys. Rev. D* 25 (1982) 2869.
- [15] Y. Yusa, et al., Belle Collaboration, *Phys. Lett. B* 589 (2004) 103.
- [16] B. Aubert, et al., BaBar Collaboration, *Phys. Rev. Lett.* 92 (2004) 121801.
- [17] B. Aubert, et al., BaBar Collaboration, *Phys. Rev. Lett.* 99 (2007) 251803.
- [18] S. Kurokawa, E. Kikutani, *Nucl. Instrum. Methods A* 499 (2003) 1, and other papers included in this volume.
- [19] A. Abashian, et al., Belle Collaboration, *Nucl. Instrum. Methods A* 479 (2002) 117.
- [20] K. Hanagaki, et al., *Nucl. Instrum. Methods A* 485 (2002) 490.
- [21] A. Abashian, et al., *Nucl. Instrum. Methods A* 491 (2002) 69.
- [22] S. Jadach, et al., *Comput. Phys. Commun.* 130 (2000) 260.
- [23] For the most general expressions for the distributions in LFV τ decays to three leptons, see the model-independent analysis of B.M. Dassing, et al., *JHEP* 0710 (2007) 039.
- [24] D.J. Lange, *Nucl. Instrum. Methods A* 462 (2001) 152.
- [25] S. Jadach, et al., *Comput. Phys. Commun.* 70 (1992) 305.
- [26] F.A. Berends, et al., *Comput. Phys. Commun.* 40 (1986) 285.
- [27] S. Brandt, et al., *Phys. Lett.* 12 (1964) 57; E. Farhi, *Phys. Rev. Lett.* 39 (1977) 1587.
- [28] K. Hayasaka, et al., Belle Collaboration, *Phys. Lett. B* 613 (2005) 20.
- [29] G.J. Feldman, R.D. Cousins, *Phys. Rev. D* 57 (1998) 3873.
- [30] See <http://www3.tsl.uu.se/~conrad/pole.html>; J. Conrad, et al., *Phys. Rev. D* 67 (2003) 012002.
- [31] S. Banerjee, et al., arXiv: 0706.3235 [hep-ph], *Phys. Rev. D*, submitted for publication.